Cell. Mol. Life Sci. 65 (2008) 3110 – 3117
1420-682X/08/193110-8
DOI 10.1007/s00018-008-8418-2

Cellular and Molecular Life Sciences

Research Article

Phosphatidylinositol 3-kinase-dependent transcriptional silencing of the translational repressor 4E-BP1

R. Azar, S. Najib, H. Lahlou[+], C. Susini and S. Pyronnet[*]

INSERM U858, Institut de Médecine Moléculaire de Rangueil, Département Cancer, BP 84225, 31432 Toulouse Cedex 4 (France), Fax: +33-561322403, e-mail: Stephane.Pyronnet@inserm.fr

Received 17 July 2008; received after revision 6 August 2008; accepted 18 August 2008
Online First 22 September 2008

Abstract. The suppressor of translation initiation *4E-BP1* functions as a key regulator in cellular growth, differentiation, apoptosis and survival. While the control of 4E-BP1 activity *via* phosphorylation has been widely studied, the molecular mechanisms and the signaling pathways that govern *4E-BP1* gene expression are largely unknown. Here we show that inactivation of phosphatidylinositol 3-kinase (PI3K) consequent to stable expression of the antiproliferative somatostatin receptor 2 (sst2) in pancreatic cancer cells leads to transcriptional accumulation of the hypophosphorylated forms of 4E-BP1 protein. In cancer cells, while *4E-BP1* gene promoter is maintained repressed in a PI3K-dependent mechanism, sst2-dependent inactivation of the PI3K/Akt pathway releases *4E-BP1* gene transcription. Furthermore, the use of a pharmacological inhibitor and dominant-negative or -positive mutants of PI3K all affect 4E-BP1 protein expression and promoter activity in different cell lines. These data show that, in addition to inactivation of 4E-BP1 *via* hyperphosphorylation, signaling through the PI3K pathway silences *4E-BP1* gene transcription.

Keywords. Translation initiation, 4E-BP1, PI3K, Egr-1, pancreatic cancer.

Introduction

The phosphatidylinositol 3-kinase (PI3K) family plays a critical role in many cellular functions including membrane trafficking, proliferation and metabolism. Among the three classes of PI3K, class I is the most documented. It is a heterodimer comprised of a p85 regulatory subunit and a p110 catalytic subunit. In response to extracellular stimuli, p85 is specifically associated with tyrosine-phosphorylated activated growth factor receptors or their substrates. Recruitment of the PI3K complex to the cell membranes activates p110, which in turn catalyzes the phosphorylation of phosphatidylinositols (PtIns). PtIns then affect both transcription and translation *via* activation of different effectors including protein kinase B (PKB/Akt), protein kinase C (PKC), serum and glucocorticoid-inducible kinase (SGK), small GTP-binding proteins like RAC1 and CDC42-dependent pathways [1].

Signaling through PI3K-Akt regulates several transcription factors implicated in cell survival and apoptosis, such as the forkhead transcription factor (FOXO). Akt phosphorylates FOXO, leading to its nuclear export and its proteasomal degradation. Akt also facilitates p53 degradation through phosphorylation of murine double minute 2 (MDM2). p53

[+] Present address: Molecular Oncology Group, McGill University, Royal Victoria Hospital, 687 Pine Av. West, Room H5.21, Montreal, QC, H3A 1A1 (Canada)
[*] Corresponding author.

inactivation amplifies the PI3K-Akt signals by decreasing the transcription of phosphatase and tensin homologue (PTEN), which negatively regulates PI3K. This positive auto-feedback loop of PI3K-Akt pathway is enhanced by the finding that the nuclear factor of κB (NF-κB) can repress PTEN promoter activity. Thus, Akt induces nuclear translocation of NF-κB by activating IKK, a kinase that allows degradation of IκB (NF-κB inhibitor). Cyclic-AMP response element-binding protein (CREB), c-MYC, β-catenin, hypoxia inducible factor 1α (HIF1α) are also targets of PI3K-Akt signaling [2]. Moreover, the other PI3K-dependent pathways feed this Akt-dependent transcription regulation.

While PI3K activates eIF2B by inhibition of glycogen synthase kinase 3 (GSK3), mammalian target of rapamycin (mTOR) remains the prominent molecule that links PI3K to protein synthesis. PI3K-Akt signal represses tuberous sclerosis complex 2 (TSC2), a tumor suppressor and a GAP for the small GTPase Rheb [3]. Since Rheb-GTP interacts with mTOR-GβL-Raptor complex (mTORC1) leading to its activation, increased Rheb-GTP level promotes protein synthesis by phosphorylation of p70 S6K (S6K) and the translation initiation factor 4E-binding protein (4E-BP1), which is a crucial regulator of translation initiation [4].

In the absence of nutrients or growth factors, 4E-BP1 is hypophosphorylated, a form that can interact with the eukaryotic initiation factor 4E (eIF4E). This interaction prevents the association of eIF4E to eIF4G and the formation of eIF4F complex, a bridge between capped mRNA and the 43S pre-initiation complex. In response to PI3K-Akt signaling, mTORC1 phosphorylates 4E-BP1 on Thr37 and Thr46 either directly (by interaction of 4E-BP1 TOS motif with raptor) or *via* other kinases associated to mTOR [5]. These phosphorylated sites are a priming event that facilitates the phosphorylation of serum-induced sites on Thr70 and Ser65, thereby abrogating the association of 4E-BP1 to eIF4E and releasing translation repression [6]. Three other sites (Ser84, Ser101 and Ser112) on 4E-BP1 have been shown to be phosphorylated, but their impacts on eIF4E interaction remain controversial [7, 8].

Here we show that the role of PI3K signaling pathway in the regulation of 4E-BP1 function is not limited to inhibition of 4E-BP1 activity *via* protein phosphorylation. Signaling through the PI3K pathway also impinges upon 4E-BP1 expression *via* Egr-1-dependent transcriptional silencing.

Materials and methods

Cell culture and drug treatments. BxPC-3 wild-type (BxPC-3), BxPC-3 mock-transfected (BxC) or stably transfected with human sst2 cDNA (Bx2), HEK-293 and BON cell lines were used in this study. Dulbecco's modified Eagle's medium (DMEM) with 1 or 4.5 g/l glucose was purchased from LONZA, other culture reagents were from GIBCO except Plasmocin and geneticin (InvivoGen). PI3K activity was inhibited using 25 μM LY294002 (Calbiochem) for 24 h.

Analysis of 4E-BP1-eIF4E interaction. BxC and Bx2 cells were harvested in lysis buffer [25 mM Tris-HCl pH 7.4, 50 mM KCL, 5 % glycerol, 0.5 % Nonidet P-40 and 1 mM DTT supplemented with protease inhibitor mixtures (Roche)]), and clarified by centrifugation at 12 000 rpm for 10 min at 4°C. The protein content was determined in the supernatant using the Bradford method (Bio-Rad). After preclearing with 10 μl Protein G-agarose-conjugate beads for 1 h at 4°C, cell lysates were subjected to immunoprecipitation as previously described [9], except that protein extracts were incubated with 10 μl eIF4E antibody-agarose conjugate (Santa Cruz Biotechnology) overnight at 4°C.

Western blotting. Cells were plated in 100-mm-diameter culture dishes (10^6 cells/dish) and grown for 24 h. After a rapid wash with ice-cold PBS, cells were harvested as described above, and Western blotting was performed as previously described [10]. Briefly, equal amounts of protein were boiled in 4× sample buffer [250 mM Tris-HCl, pH 6.8, 8 % sodium dodecyl sulfate (SDS), 20 % 2-mercaptoethanol, 50 % glycerol, bromophenol blue]. Samples were separated by SDS-polyacrylamide gel electrophoresis (SDS-PAGE) followed by electrophoretic transfer onto nitrocellulose membranes (Pall Life Sciences). Membranes were incubated with: mouse monoclonal antibodies to β-tubulin (Sigma), phospho-specific p38 and phospho-specific ERK1/2 (cell signaling); rabbit polyclonal antibody against eIF4G-I was kindly provided by N. Sonenberg (Department of Biochemistry and McGill Cancer Center, McGill University), ERK2, p38 and egr-1 (Santa Cruz Biotechnology), phospho-JNK (Thr183/Tyr185), JNK, phospho-Akt (ser473), Akt, eIF4E, total and phospho-specific 4E-BP1 (cell signaling). Membranes were then subjected to immunoblotting using goat horseradish peroxidase-conjugated secondary antibodies to mouse or rabbit IgG (Pierce). Peroxidase activity was revealed using the enhanced chemiluminescence (ECL) system (Pierce). Quantitative analyses were carried out by using Phoretix 1D software (Samba technologies).

Table 1. Primers for plasmid constructions and chromatin immunoprecipitation (ChIP) assay.

Construction Plasmid name	Forward primer	Reverse primer
-960/+64	5' ggggtaccgcctcaaacccctgggct 3'	5' tccgctcgaggtctcctgtgcgctgcac 3'
-628/+64	5' ggggtaccaacgcccttccccaccac 3'	5' tccgctcgaggtctcctgtgcgctgcac 3'
-278/+64	5' ggggtaccattaatttaggcgagcta 3'	5' tccgctcgaggtctcctgtgcgctgcac 3'
-160/+64	5' ggggtaccagcccgtgagcagacggg 3'	5' tccgctcgaggtctcctgtgcgctgcac 3'
-278/-1	5' ggggtaccattaatttaggcgagcta 3'	5' accgctcgagctcgccccgtcccgcccc 3'
-160/-1	5' ggggtaccagcccgtgagcagacggg 3'	5' accgctcgagctcgccccgtcccgcccc 3'
-219/-123	5' ggggtaccacggaggggcagtcgctg 3'	5' accgctcgagggatttgtagtccgcgcc 3'
-278/-142	5' ggggtaccattaatttaggcgagcta 3'	5' accgctcgagcccgtctgctcacgggct 3'
-960/-260	5' ggggtaccgcctcaaacccctgggct 3'	5' accgctcgagtagctcgcctaaattaat 3'
-628/-260	5' ggggtaccaacgcccttccccaccac 3'	5' accgctcgagtagctcgcctaaattaat 3'
-960/-610	5' ggggtaccgcctcaaacccctgggct 3'	5' accgctcgaggtggtggggaagggcgtt 3'
ChIP assay		
Sequence		
-160/+64	5' agcccgtgagcagacgggagt 3'	5' ggtctcctgtgcgctgcaccc 3'
-960/-610	5' gcctcaaacccctgggctcaa 3'	5' gtggtggggaagggcgttgga 3'

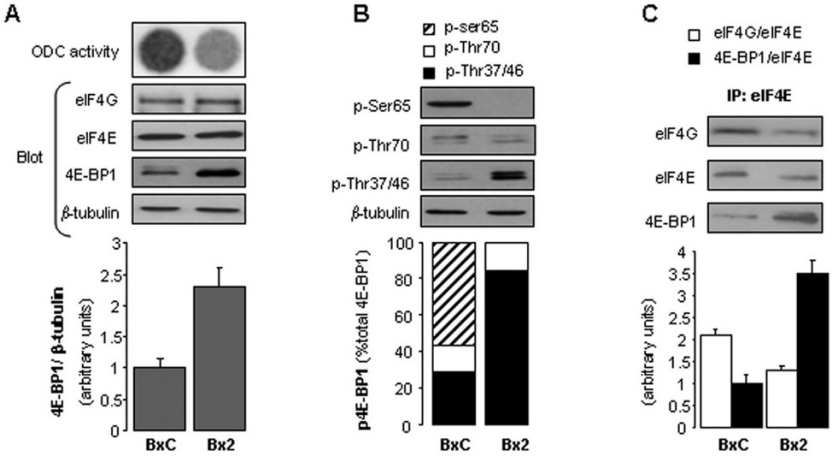

Figure 1. Inhibition of cap-dependent translation in somatostatin receptor 2 (sst2)-expressing cells. (*A*) Ornithine decarboxylase (ODC) activity was measured in growing cells (top). Immunoblotting of equal amounts of proteins using specific antibodies was performed as indicated (middle). Histograms represent the amount of 4E-BP1 normalized to β-tubulin. They are the means ± SEM of three separate experiments, and are relative to the value obtained for BxC cells and which was set at 1 (bottom). (*B*) Immunoblotting of equal amounts of proteins using specific antibodies was performed as indicated (top). Histograms represent the proportions of 4E-BP1 that are phosphorylated at each site, as indicated (top). Results are representative of three separate experiments (bottom). (*C*) Immunoblotting of proteins following eukaryotic initiation factor 4E (eIF4E) immunoprecipitation using specific antibodies was performed as indicated (top). Histograms represent the ratio of eIF4G or 4E-BP1 to eIF4E amounts and are normalized to the ratio obtained with 4E-BP1 and eIF4E in BxC cells, which was set at 1. They are the means ± SEM of three separate experiments (bottom).

***In vivo* labeling, protein synthesis and ornithine decarboxylase assay.** Cells were plated in 60-mm-diameter culture dishes (4×10^5 cells/dish) and grown for 2 days. Cells were starved for methionine for 30 min at 37°C in methionine-free DMEM and supplemented with 7.5 % FCS and 2 mM glutamine. The medium was then replaced with fresh methionine-free medium containing [^{35}S]methionine (10 μCi/ml) from Amersham Biosciences. The radioactive medium was removed after a 30-min pulse, and cells were rinsed twice with ice-cold PBS. Cells were then lysed at 4°C in lysis buffer as described above, and protein content was quantified. Equal amounts were either immunoprecipitated using polyclonal antibodies directed against 4E-BP1 (Cell signaling) or directly dissolved in 4× sample buffer as described [11].

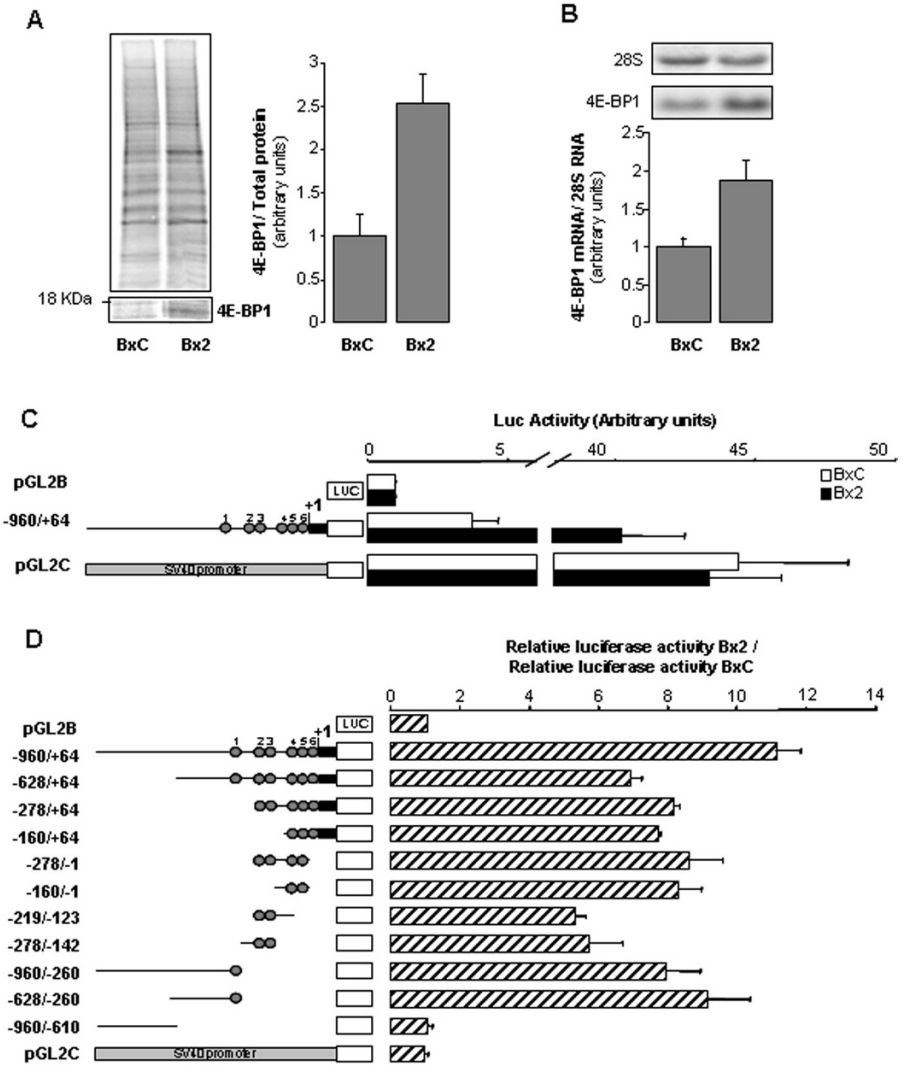

Figure 2. 4E-BP1 induction by sst2 is transcriptional. (*A*) Following pulse-labeling of cells (left), [^{35}S]methionine incorporation into total protein (top) or into immunoprecipitated 4E-BP1 protein (bottom) was visualized by autoradiography, as described in Methods. Histograms represent the amount of 4E-BP1 normalized to [^{35}S]methionine incorporation into total protein and are the means ± SEM of three separate experiments expressed relative to the value obtained for BxC cells, which was set at 1 (right). (*B*) Total RNA was subjected to Northern blotting as described in Methods (top), and quantified, normalized to 28S RNA and expressed as described in (*A*) (bottom). (*C*) Luciferase (LUC) activity was assayed 36 h following BxC or Bx2 cells transfection. Transfection efficiency was normalized to the concurrent transfection of a CMV-*Renilla* luciferase reporter plasmid. Luciferase activities are represented as the means ± SEM of three independent experiments performed in triplicates. They are relative to the luciferase activity obtained for pGL2B (devoid of promoter sequence) and which was set at 1. Sequences inserted upstream from luciferase (open rectangles) were as follows. Thin line: 4E-BP1 gene sequence upstream form the +1 transcription start site; thick line: 4E-BP1 gene sequence located between the +1 transcription start site and the AUG initiator codon (5' UTR); filled small circles: computer-predicted Egr-1 responsive elements (numbered 1–6); gray rectangle: SV40 promoter. (*D*) Luciferase activity was assayed 36 h following transfection. Transfection efficiency was normalized to the concurrent transfection of a CMV-*Renilla* luciferase reporter plasmid. Histograms are representative of three independent experiments performed in triplicates. They represent the ratio between luciferase activities measured in Bx2 cells and luciferase activity measured in BxC cells, and are relative to the ratio obtained for pGL2B.

Ornithine decarboxylase (ODC) activity was determined as described previously [12]. Briefly, cells were scraped in lysis buffer (0.25 M Tris-HCl pH 7.4, 1 mM EDTA, 1 mM DTT), and subjected to two freeze-thaw cycles. The lysate was centrifuged at 14 000 rpm for 10 min to remove cellular debris. Equal amounts of total protein (50 µg) were incubated with 2.5 µCi [^{14}C]ornithine (Amersham) and 50 µM pyridoxal 5-phosphate for 1 h at 37°C. Incubations were performed in 96-well microtiter plates. Liberated $^{14}CO_2$ was trapped in a covering 3MM paper saturated with a solution of barium hydroxide. The dried 3MM paper was exposed to an X-ray film.

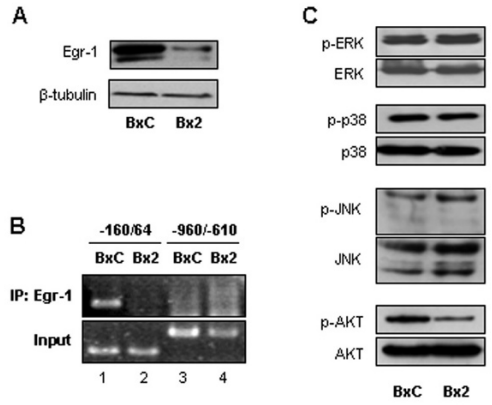

Figure 3. A link between Egr-1, 4E-BP1 promoter and PI3K signaling. (*A*) Immunoblotting of equal amounts of proteins using specific antibodies was performed as indicated. (*B*) Chromatin immunoprecipitation (ChIP) using Egr-1 specific antibodies was performed using fragments that contain computer-predicted Egr-1-responsive elements (–160/64) or not (–960/–610) as indicated. Primers' specificity and efficacy have been validated by amplification of genomic DNA (input). (*C*) Equal amounts of proteins were subjected to immunoblotting using specific antibodies as indicated.

RNA isolation and Northern blotting. Total RNA was isolated using RNeasy Kit (Qiagen) according to the manufacturer's instructions. From the total RNA, 10 μg was denaturated in RNA sample buffer (39 mM MOPS pH 7, 58.5 % deionized formamide, 10.8 % formaldehyde, 3 % ethidium bromide) for 15 min at 65°C, separated by electrophoresis on agarose formaldehyde gels, and transferred to a nylon membrane (Hybond^{TM}-N^{+}; Amersham Biosciences) by capillary transfer in a 10× SSC buffer (Invitrogen). After UV-cross linking (Cross-linker; Stratagene) and prehybridization for 2 h at 68°C with QuikHyb® (Stratagene), filters were hybridized for 3 h with ^{32}P-labeled probes made from the agarose gel-purified RT-PCR products of each gene using the RadPrime DNA Labeling System (Invitrogen) and 10 μg salmon sperm DNA (Stratagen). After washing, hybridized membranes were exposed to a PhosphorImager (Molecular Dynamics). Equal loading of RNA was confirmed by staining of the ribosomal RNA with ethidium bromide. Signals were quantified using the ImageQuant software (Amersham).

Luciferase reporter gene analysis. To determine 4E-BP1 promoter activity, the dual-luciferase reporter assay system (Promega) was used. In brief, cells (10^5 cells/well) were plated in six-well plates, transiently transfected with pGL2-control vector (pGL2C), pGL2-Basic vector (pGL2C) or human 4E-BP1 promoter sequences-firefly luciferase constructs and pCMV-Renilla luciferase plasmid (Promega) using Exgen 500 (Euromedex). pGL2-B, full-length 4E-BP1 promoter construct and pGL2-C were kindly provided by M. Rolli-Derkinderen. Fragments of 4E-BP1 promoter were PCR-amplified using primers extended by *Kpn*I (forward primers) and by *Xho*I (reverse primers) restriction sites (see primers listed in Table 1), digested by *Kpn*I/*Xho*I restriction endonucleases and inserted into *Kpn*I/*Xho*I-linearized pGL2B. The pCMV-Renilla luciferase plasmid was used to evaluate transfection efficiency. Transfected cells were incubated in normal culture medium for 36 h, and harvested in Passive Lysis Buffer (Promega). Extracts were assayed for firefly and Renilla luciferase activities and detected with Centro LB 960 (Berthold Technologies). The relative luciferase activity was calculated by normalizing firefly luciferase activity to that of Renilla luciferase activity.

Chromatin immunoprecipitation (ChIP) analysis. Experiments were performed using EZ ChIP^{TM} assay kit (Upstate Biotechnology) according to the manufacturer's instructions. Immunoprecipitation was processed using mouse monoclonal antibody against egr-1 (Santa Cruz) and PCR amplification was performed using the primers listed in Table 1.

Results and discussion

We have previously shown that the regulation of translation initiation plays a critical role in the inhibition of pancreatic cancer cell (BxPC3) proliferation by stable expression of the somatostatin receptor 2 (sst2) [11]. sst2 induces IRES-dependent translation initiation of connexin 26 and 43 mRNAs, and connexins assemble into functional intercellular gap junctions that restore density-dependent inhibition of cell proliferation. This paper also suggested that changes in cap- or IRES-dependent translation initiation could result from modifications of the translational repressor 4E-BP1. However, the nature of 4E-BP1 modifications and the molecular mechanisms responsible for 4E-BP1 changes were not elucidated. To clarify how sst2 can control 4E-BP1 activity, we first searched whether 4E-BP1 phosphorylation and/or expression, and therefore cap-dependent translation, could be altered in sst2-expressing cells. One protein whose expression is considered as sensitive to changes in 4E-BP1 activity in pancreatic cancer cells is ODC [13]. As expected, ODC activity (which generally reflects ODC protein amount) was much lower in cells that express sst2 (Fig. 1A, top). This was consistent with the observation that 4E-BP1 amount was in contrast higher in sst2-expressing cells, while the amounts of eIF4E and eIF4G and that of β-tubulin (which was used as a

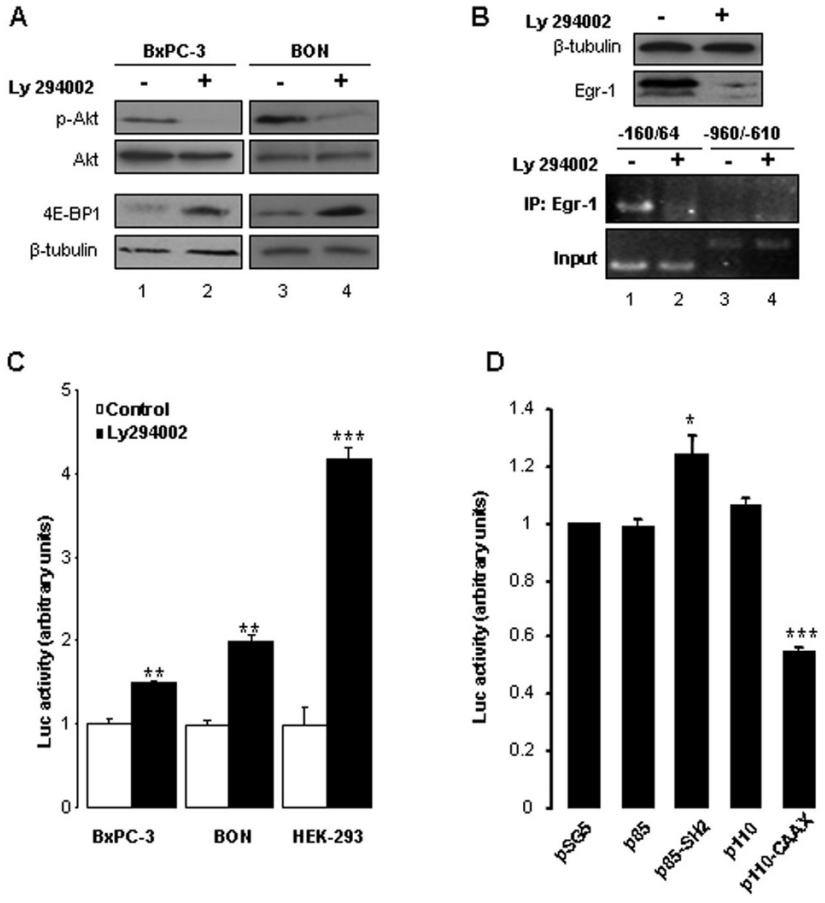

Figure 4. PI3K controls 4E-BP1 promoter. (*A*) Equal amounts of proteins from cells untreated or treated with LY294002 for 24 h were subjected to immunoblotting using specific antibodies as indicated. (*B*) Equal amounts of proteins from cells untreated or treated with LY294002 were subjected to immunoblotting using specific antibodies as indicated (top). ChIP using Egr-1 specific antibodies was performed as described in Fig. 3B (bottom). (*C*) Cells were untreated or treated with LY294002 36 h following transfection, and luciferase activity was assayed as described in Methods. Transfection efficiency was normalized to the concurrent transfection of a CMV-*Renilla* luciferase reporter plasmid. Histograms represent the means ± SEM of three independent experiments performed in triplicates. They are expressed as the ratio between luciferase activities measured in the presence of LY294002 and luciferase activities measured in the absence of LY294002 (which were set at 1 for each cell line). (*D*) Luciferase activity was assayed 36 h following co-transfection of HEK cells with –960/+64 4E-BP1 promoter and pSG5 (mock) or p85 (wild-type p85), p-85-SH2 (an inactive form of p85), p110 (wild-type p110α) or p110-CAAX (a constitutively active form of p110α) plasmids, as indicated. Transfection efficiency was normalized to the concurrent transfection of a CMV-Renilla luciferase reporter plasmid. Histograms represent the means ± SEM of three independent experiments performed in triplicates. They are relative to the value obtained for mock (psG5) transfected cells and which was set at 1. *t*-test: * $p<0.05$; ** $p<0.01$; *** $p<0.005$.)

loading control) were similar in both cell lines (Fig. 1A, bottom). Furthermore, the use of 4E-BP1 phospho-specific antibodies showed that Ser65 (and to a lesser extent Thr70) were hypophosphorylated in sst2-expressing cells, while the signal detected with p-Thr37/46 antibodies perfectly reflected that of total 4E-BP1, indicating that phosphorylations at Thr37 or Thr46 were not regulated by sst2 (Fig. 1B). As expected, increased levels of 4E-BP1 and hypophosphorylations of Ser65 and Thr70 resulted in increased binding of 4E-BP1 to eIF4E but were detrimental to eIF4G association with eIF4E in sst2-expressing cells (Fig. 1C). These data indicate that sst2 is capable of inhibiting eIF4F assembly (and therefore cap-dependent translation) *via* hypophosphorylation and accumulation of 4E-BP1 protein.

We have previously shown that, in BxPC3 cells stably expressing sst2, PI3K is inhibited as a consequence of direct binding of the regulatory p85 subunit to the receptor [14], and it is well established that 4E-BP1 phosphorylation is under the control of the PI3K-Akt/mTOR-signaling pathway. We therefore decided not to continue our investigations on the regulation of 4E-BP1 phosphorylation but instead to focus our attention on the intriguing observation that 4E-BP1 expression was regulated by sst2. We first determined the molecular step at which 4E-BP1 expression could be controlled by sst2. While treatment of cells with

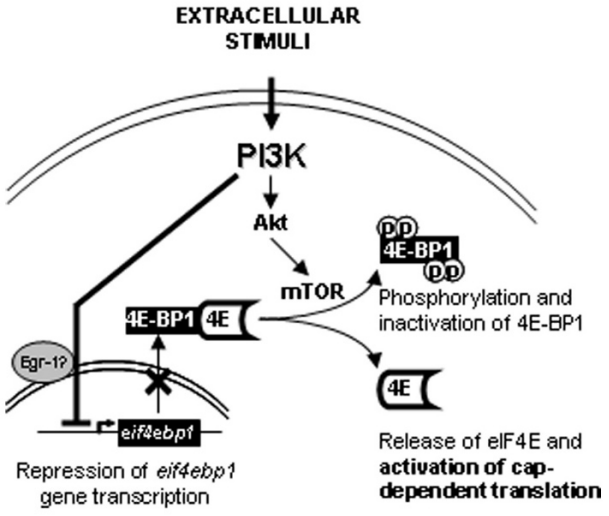

Figure 5. PI3K controls cap-dependent translation through 4E-BP1 phosphorylation and transcription. Following PI3K activation by extracellular stimuli, 4E-BP1 gene (eif4ebp1) transcription is repressed (possibly through Egr-1) and induction of the Akt/mTOR pathway leads to 4E-BP1 phosphorylation. Consequently, sequestered eIF4E (4E) is released and can serve for cap-dependent translation initiation.

cycloheximide showed that sst2 had no effect on 4E-BP1 protein half-life (data not shown), a pulse-labeling of cells revealed that 4E-BP1 *de novo* synthesis was, however, up-regulated in sst2-expressing cells (Fig. 2A). Similarly, treatment with actinomycin-D showed that sst2 had no effect on 4E-BP1 mRNA half-life (data not shown), while a Northern blot analysis revealed that 4E-BP1 mRNA level was higher in sst2-expressing cells (Fig. 2B). To ensure that such higher amount of 4E-BP1 mRNA was actually a consequence of increased transcription rate of 4E-BP1 gene, the promoter of 4E-BP1 was tested in a luciferase reporter assay. As compared to a vector devoid of promoter sequence (pGL2B), a vector carrying a –960/+64 4E-BP1 promoter fragment permitted efficient luciferase expression in pancreatic BxPC3 cells, although it was weaker than the SV40 promoter, which was used as a positive control (Fig. 2C). These data also revealed that 4E-BP1 promoter was much more active in sst2-expressing cells and that sst2 specifically targeted 4E-BP1 promoter as SV40 promoter activity was independent of sst2 expression (Fig. 2C).

To go further in the delineation of the promoter fragment, and hence in the identification of the transcription factor, which could be involved in sst2-dependent regulation of 4E-BP1 expression, a series of 4E-BP1 promoter deletion mutants has been generated, and tested in a luciferase reporter assay. Intriguingly, it was not possible to identify a unique promoter fragment that contained all the requirements for regulation by sst2. However, all 4E-BP1 promoter segments possessing at least one GC-rich Egr-1-responsive element were sensitive to sst2 expression (Fig. 2D). None of the six GC-rich Egr-1 putative elements (numbered 1–6 in Fig. 2D) was prominent as they all contributed to sst2 effect on 4E-BP1 promoter. Conversely, the unique fragment lacking Egr-1-responsive element (–960/–610) did not respond to sst2. These data demonstrate that 4E-BP1 promoter activity is enhanced in sst2-expressing pancreatic cancer cells, and that the transcription factor Egr-1 is a probable candidate involved in such regulation.

Egr-1 is an "early growth response gene" encoding a transcription factor that has been shown to silence 4E-BP1 promoter activity following activation of the MAPK signaling pathway in hematopoietic cell lines [15]. Consistently, Egr-1 is overexpressed in pancreatic cells that do not express sst2 (Fig. 3A). Furthermore, a ChIP assay revealed that a fragment of endogenous 4E-BP1 promoter that contains several Egr-1-responsive elements can be immunoprecipitated by anti-Egr-1-specific antibodies much more efficiently in cells lacking sst2 (Fig. 3B, compare lane 1 to lane 2), while a fragment lacking Egr-1-responsive element cannot (lanes 3 and 4). The regulation of Egr-1 expression in pancreatic cancer cells could not be attributed to changes in MAPK activity, as sst2 had no effect on Erk1/2, p38 or JNK phosphorylation (Fig. 3C). However, the fact that Akt phosphorylation was inhibited in sst2-expressing cells (Fig. 3C), and that we have shown that PI3K is inhibited in BxPC3 cells as a consequence of direct binding of the regulatory p85 subunit to sst2 [14], suggested that 4E-BP1 expression could be regulated by the PI3K pathway. This suggestion was further supported by earlier papers reporting that Egr-1 expression can be targeted by PI3K signaling following activation of other G protein-coupled receptors [16, 17].

We therefore anticipated that 4E-BP1 transcription could be maintained repressed by the PI3K signaling pathway in pancreatic cancer cells, and that sst2 could release 4E-BP1 expression as a consequence of PI3K inhibition. As expected, pharmacological inhibition of PI3K activity by LY294002, attested by inhibition of Akt phosphorylation, increased 4E-BP1 protein level (Fig. 4A, compare lane 1 to lane 2). PI3K inhibition also provoked a decrease in Egr-1 expression which was accompanied by a corresponding decrease in the amount of Egr-1 bound to endogenous 4E-BP1 promoter (Fig. 4B), and a corresponding increase in 4E-BP1 promoter activity (Fig. 4C, BxPC3 cells). Furthermore, the implication of PI3K signaling in the regulation of 4E-BP1 transcriptional expression was not limited to exocrine pancreatic cells as treat-

ment with LY294002 enhanced 4E-BP1 protein expression in cells originating from human pancreatic endocrine tumors (Fig. 4A, BON cells), and enhanced 4E-BP1 promoter activity in BON cells (Fig. 4C, BON cells), and in cells originating from human embryonic kidney (Fig. 4C, HEK cells).

Finally, 4E-BP1 promoter activity could be either enhanced by the use of a dominant negative mutant of the p85α regulatory subunit (p85-SH2) or inhibited by the use of a constitutively active mutant of the catalytic p110α subunit (p110-CAAX) of PI3K (Fig. 4D), thus indicating that PI3Kα subunits are involved in 4E-BP1 regulation. These tests were also performed to ensure that the effects obtained with LY294002 were not due to nonspecific inactivation of other kinases such as PI4K.

Taken together, these data demonstrate that, in addition to 4E-BP1 inactivation by phosphorylation, signaling through PI3K pathway also impinges upon 4E-BP1 amount *via* transcriptional silencing (Fig. 5). Egr-1 appears as a good candidate involved in PI3K-dependent repression of 4E-BP1 gene transcription. Because 4E-BP1 expression has been shown to be down-regulated in many high-grade tumors and since PI3K activity is often enhanced in cancer cells, it would be interesting to determine whether 4E-BP1 loss in tumors is due to higher PI3K activity. Finally, it is probable that PI3K can regulate 4E-BP1 transcription through other transcription factors. This speculation can be deduced from two reports showing that in Drosophila 4E-BP1 transcription is under the control of FOXO [18], a forkhead transcription factor which is itself controlled by PI3K signaling [19].

Acknowledgements. We thank M. Rolli-Derkinderen for 4E-BP1 promoter sequence, B. Vanhaesebroeck for p85 and p110 constructs and N. Sonenberg for eIF4GI antibody. This work was funded by grants from INSERM, from La Ligue Contre le Cancer, from Cancéropôle Grand-Sud-Ouest and from Association pour la Recherche sur le Cancer (ARC). R. Azar was a recipient of fellowships from ARC, from Fondation pour la Recherche Médicale (FRM), from Agence Universitaire de la Francophonie (AUF).

1 Hennessy, B. T., Smith, D. L., Ram, P. T., Lu, Y. and Mills, G. B. (2005) Exploiting the PI3K/AKT pathway for cancer drug discovery. Nat. Rev. Drug Discov. 4, 988–1004
2 Bader, A. G., Kang, S., Zhao, L. and Vogt, P. K. (2005) Oncogenic PI3K deregulates transcription and translation. Nat. Rev. Cancer 5, 921–929
3 Stocker, H., Radimerski, T., Schindelholz, B., Wittwer, F., Belwat, P., Daram, P., Breuer, S., Thomas, G. and Hafen, E. (2003) Rheb is an essential regulator of S6K in controlling cell growth in *Drosophila.* Nat. Cell Biol. 5, 559–565
4 Long, X., Lin, Y., Ortiz-Vega, S., Yonezawa, K. and Avruch, J. (2005) Rheb binds and regulates the mTOR kinase. Curr. Biol. 15, 702–713
5 Wang, X., Beugnet, A., Murakami, M., Yamanaka, S. and Proud, C. G. (2005) Distinct signaling events downstream of mTOR cooperate to mediate the effects of amino acids and insulin on initiation factor 4E-binding proteins. Mol. Cell. Biol. 25, 2558–2572
6 Gingras, A. C., Raught, B., Gygi, S. P., Niedzwiecka, A., Miron, M., Burley, S. K., Polakiewicz, R. D., Wyslouch-Cieszynska, A., Aebersold, R. and Sonenberg, N. (2001) Hierarchical phosphorylation of the translation inhibitor 4E-BP1. Genes Dev. 15, 2852–2864
7 Ferguson, G., Mothe-Satney, I. and Lawrence. J. C. (2003) Ser-64 and Ser-111 in PHAS-I are dispensable for insulin-stimulated dissociation from eIF4E. J. Biol. Chem. 278, 47459–47465
8 Wang, X., Li, W., Parra, J. L., Beugnet, A. and Proud, C. G. (2003) The C terminus of initiation factor 4E-binding protein 1 contains multiple regulatory features that influence its function and phosphorylation. Mol. Cell. Biol. 23, 1546–1557
9 Pyronnet, S., Dostie, J. and Sonenberg, N. (2001) Suppression of cap-dependent translation in mitosis. Genes Dev. 15, 2083–2093
10 Pyronnet, S., Imataka, H., Gingras, A. C., Fukunaga, R., Hunter, T. and Sonenberg, N. (1999) Human eukaryotic translation initiation factor 4G (eIF4G) recruits mnk1 to phosphorylate eIF4E. EMBO J. 18, 270–279
11 Lahlou, H., Fanjul, M., Pradayrol, L., Susini, C. and Pyronnet, S. (2005) Restoration of functional gap junctions through internal ribosome entry site-dependent synthesis of endogenous connexins in density-inhibited cancer cells. Mol. Cell. Biol. 25, 4034–4045
12 Pyronnet, S., Pradayrol, L. and Sonenberg, N. (2000) A cell cycle-dependent internal ribosome entry site. Mol. Cell. 5, 607–616
13 Pyronnet, S., Gingras, A. C., Bouisson, M., Kowalski-Chauvel, A., Seva, C., Vaysse, N., Sonenberg, N. and Pradayrol, L. (1998) Gastrin induces phosphorylation of eIF4E binding protein 1 and translation initiation of ornithine decarboxylase mRNA. Oncogene 16, 2219–2227
14 Bousquet, C., Guillermet-Guibert, J., Saint-Laurent, N., Archer-Lahlou, E., Lopez, F., Fanjul, M., Ferrand, A., Fourmy, D., Pichereaux, C., Monsarrat, B., Pradayrol, L., Estève, J. P. and Susini, C. (2006) Direct binding of p85 to sst2 somatostatin receptor reveals a novel mechanism for inhibiting PI3K pathway. EMBO J. 25: 3943–3954
15 Rolli-Derkinderen, M., Machavoine, F., Baraban, J. M., Grolleau, A., Beretta, L. and Dy, M. (2003) ERK and p38 inhibit the expression of 4E-BP1 repressor of translation through induction of Egr-1. J. Biol. Chem. 278, 18859–18867
16 Guillemot, L., Levy, A., Raymondjean, M. and Rothhut, B. (2001) Angiotensin II-induced transcriptional activation of the cyclin D1 gene is mediated by Egr-1 in CHO-AT(1A) cells. J. Biol. Chem. 276, 39394–39403
17 Fujino, H., Xu, W. and Regan, J. W. (2003) Prostaglandin E2 induced functional expression of early growth response factor-1 by EP4, but not EP2, prostanoid receptors *via* the phosphatidylinositol 3-kinase and extracellular signal-regulated kinases. J. Biol. Chem. 278, 12151–12156
18 Tettweiler, G., Miron, M., Jenkins, M., Sonenberg, N. and Lasko, P. F. (2005) Starvation and oxidative stress resistance in Drosophila are mediated through the eIF4E-binding protein, d4E-BP. Genes Dev. 19, 1840–1843
19 Puig, O., Marr, M. T., Ruhf, M. L. and Tjian, R. (2003) Control of cell number by Drosophila FOXO: Downstream and feedback regulation of the insulin receptor pathway. Genes Dev. 17, 2006–2020